The Journal of Neuroscience, August 1, 1999, *19*(15):6475–6487

Ultrastructural Localization of the α4-Subunit of the Neuronal Acetylcholine Nicotinic Receptor in the Rat Substantia Nigra

Maria del Mar Arroyo-Jiménez,[1,2,3] Jean-Pierre Bourgeois,[1] Lisa M. Marubio,[1] Anne-Marie Le Sourd,[1] Ole Petter Ottersen,[4] Eric Rinvik,[4] Alfonso Fairén,[2,3] and Jean-Pierre Changeux[1]

[1]*Neurobiologie Moléculaire, Unité Associée Centre National de la Recherche Scientifique D1284, Département des Biotechnologies, Institut Pasteur, 75724 Paris Cedex 15, France,* [2]*Instituto Cajal, Consejo Superior de Investigaciones Científicas, 28002 Madrid, Spain,* [3]*Instituto de Neurociencias, Universidad Miguel Hernández, 03550 San Juan de Alicante, Spain, and* [4]*Department of Anatomy, Institute of Basic Medical Sciences, University of Oslo, Blindern N-0317, Oslo, Norway*

The distribution of the α4-subunit of the neuronal nicotinic acetylcholine receptor (nAChR) in the rat brain was examined at light and electron microscopy levels using immunohistochemical staining. In the present study we demonstrate the specificity, in both tissue homogenates and brain sections, of a polyclonal antibody raised against the rat nAChR α4-subunit. The characterization of this antibody involved: (1) Western blot analysis of rat brain homogenates and membrane extracts from cells previously transfected with diverse combinations of neuronal nAChR subunits, and (2) immunohistochemistry using transfected cells and rat brain tissue.

At the light microscope level, the α4-subunit-like-immunoreactivity (LI) was widely distributed in the rat brain and matched the distribution of the α4-subunit transcripts observed previously by *in situ* hybridization. Strong immunohistochemical labeling was detected in the mesencephalic dopaminergic nuclei. The nAChRs in this region are thought to be responsible for the modulation of dopaminergic transmission. The neurotransmitter identity of α4-immunolabeled neurons in the substantia nigra pars compacta (SNpc) and the ventral tegmental area was thus assessed by investigating the possible colocalization of the nAChR α4-subunit with tyrosine hydroxylase using confocal microscopy. The double labeling experiments unambiguously indicated that the α4-subunit-LI is present in dopaminergic neurons.

At the electron microscope level, the neurons in the SNpc exhibited α4-subunit-LI in association with a minority of postsynaptic densities, suggesting that the α4-subunit may be a component of functional nAChRs mediating synaptic transmission between midbrain cholinergic neurons and mesencephalic dopaminergic neurons.

Key words: neuronal nAChR; immunohistochemistry; immunogold; postsynaptic localization; substantia nigra; dopaminergic nuclei; rat brain

The nicotinic acetylcholine receptor (nAChR) is a pentameric protein that forms a cation-selective channel at the neuromuscular junction (Changeux, 1991) and in the peripheral nervous system and CNS (Sargent, 1993). In rat brain, the neuronal nAChRs comprise at least six α subunits, named α2–α7, and three β subunits named β2–β4 (Le Novère and Changeux, 1995). Both types of subunits can contribute to the various pharmacological profiles of neuronal nAChRs and may form a number of functionally different hetero-oligomers (Boulter et al., 1987; Luetje and Patrick, 1991; Conroy et al., 1992; Vernallis et al., 1993; Bertrand and Changeux, 1995; Conroy and Berg, 1995; Ramirez-Latorre et al., 1996; Role and Berg, 1996; Wang et al., 1996; Ragozzino et al., 1997).

In situ hybridization (ISH) studies revealed that the neuronal nAChR subunits mRNAs display diverse, yet overlapping expression patterns in the CNS (Wada et al., 1989, 1990; Duvoisin et al., 1989; Dineley-Miller and Patrick, 1992; Seguela et al., 1993). Immunohistochemistry provides further information on the topological distribution of neuronal nAChR protein subunits at the cellular and subcellular levels. Neuronal nAChRs have been mapped using a variety of antibodies on tissue sections of rat brain (Mason, 1985; Swanson et al., 1987; Schroder et al., 1989; Bravo and Karten, 1992; Okuda et al., 1993; Dominguez del Toro et al., 1994; Nakayama et al., 1995; Goldner et al., 1997; Rogers et al., 1998; Sorenson et al., 1998). For instance, the staining patterns obtained using antibodies against the β2-subunit (Deutch et al., 1987; Hill et al., 1993) parallel those observed with [^{3}H]nicotine and [^{3}H]acetylcholine (ACh) binding (Clarke et al., 1985b).

Several lines of evidence indicate that activation of the mesotelencephalic dopaminergic systems is involved in the reinforcing properties of nicotine (Imperato et al., 1986; Corrigall et al., 1992; Pontieri et al., 1996) as well as of several other drugs of abuse, such as opiates, cocaine, amphetamine, and ethanol (Koob, 1992,

Received August 7, 1998; revised May 14, 1999; accepted May 14, 1999.

This research was supported by grants from The Collège de France, the Association Française contre la Myopathie, the Council for Tobacco Research, Reynolds Pharmaceutics, the European Union (Biomed BMH1-CT94–1060 and Biotech 960236), the French Embassy in Spain, the Ministerio de Educacion y Cultura (PB94–0219-CO2-01), the Comunidad de Madrid (AE00268/95), and the National Alliance for Research on Schizophrenia and Depression. We are grateful to Dr. Y. Pass for his kind and qualified help in several experiments. We are indebted to Dr. P. J. Corringer, S. Bohler for scientific discussions and materials provided, and Drs. R. Miles, M. Zoli, C. Léna, and N. Le Novère for critical reading of this manuscript. We thank P. Gounon, director of the Station Centrale de Microscopie Electronique at Institut Pasteur, and K. M. Gujord at Oslo University for their constant and expert advice during all this work. We would also to thank R. Hellio, B. Martín-Clemente, and Dr. J. R Martínez-Galán for their help in confocal microscopy.

Correspondence should be addressed to Jean-Pierre Changeux, Neurobiologie Moléculaire, Département des Biotechnologies, Institut Pasteur, 25, rue du Dr. Roux, 75724 Paris Cedex 15, France.

Dr. M. del Mar Arroyo-Jiménez's present address: Facultad de Medicina, Universidad de Castilla–La Mancha, Edificio Benjamín Palencia, Campus Universitario, 02071 Albacete, Spain.

1996). In the case of nicotine, activation of dopaminergic systems is thought to be principally mediated by nAChRs located in the mesencephalon (Nisell et al., 1994). Indeed, electrophysiological experiments have shown that nicotine can activate dopaminergic (DA) neurons in preparations of rodent mesencephalon (Clarke et al., 1985a; Pidoplichko et al., 1997; Picciotto et al., 1998; Sorenson et al., 1998).

Little information is available, however, on the exact cellular localization and subunit composition of the nAChRs responsible for the effects of nicotine. Neurochemical-selective lesions in rats indicated that[^{3}H]nicotine binding sites are specifically associated with DA neurons (Clarke and Pert, 1985; Clarke et al., 1985b). Also [^{3}H]cytisine labeling, another high-affinity agonist at nicotinic receptors, was found on DA neurons (Happe et al., 1994). Antibodies against the α4-subunit were able to immunoprecipitate receptors labeled either by [^{3}H]nicotine (Whiting and Lindstrom, 1987, 1988) or [^{3}H]cytisine (Flores et al., 1992) binding. The substantia nigra pars compacta (SNpc) and ventral tegmental area (VTA) contain moderate to high levels of the α3, α4, α5, α6, β2, and β3 nAChR-subunit mRNAs (Wada et al., 1989, 1990; Deneris et al., 1989; Dineley-Miller and Patrick, 1992; Le Novère et al., 1996).

Electrophysiological experiments have shown that nAChRs with putative α4–β2 and α7 compositions are present on DA cell bodies of the rodent mesencephalon (Pidoplichko et al., 1997; Picciotto et al., 1998; Sorenson et al., 1998). Neurochemical studies further suggest the existence of α3- or α6-containing nAChRs on DA nerve terminals (for discussion, see Le Novère et al., 1996).

We demonstrate here the colocalization of tyrosine hydroxylase (TH) and α4-subunit-like-immunoreactivity (LI) in mesencephalic DA neurons and provide new ultrastructural data using both immunoperoxidase and immunogold techniques on the subcellular localization of α4-containing nAChRs in the SNpc.

MATERIALS AND METHODS

Antibodies. We used a polyclonal antibody (catalog #1772, lot #D256; Santa Cruz Biotechnology, Santa Cruz, CA) raised in goat against a synthetic peptide corresponding to a portion of the intracellular domain of the rat (*Rattus norvegicus*) nAChR α4-subunit. The immunogenic peptide is a 20 amino acid sequence comprising residues 573–592 of the cDNA deduced sequence α4-subunit (RAVEGVQYIADHLKAEDTDF), which corresponds to the highly variable cytoplasmic loop between the membrane-spanning domains M3 and M4. This antibody should recognize both identified splice variants, α4–1 and α4–2, because the sequence used for immunization is localized upstream from the splicing region of the cDNA sequence according to Goldman et al. (1987).

The specificity of this antibody was assessed by several methods in both tissue homogenates and sections.

Western blot analysis in rat homogenates. Whole extracts from three rat brains and lungs were analyzed separately by six Western blots. Tissues were homogenized in five volumes of boiling lysis buffer (1% SDS, 10 mM Tris-HCl, pH 7.4) and centrifuged at 550 × *g* for 10 min. Supernatant was collected, aliquoted, and frozen at −80°C until use.

Fifty microgram aliquots of either sample were separated by SDS-PAGE (10% gels). Proteins were transferred to nitrocellulose membranes, blocked overnight with 5% nonfat dry milk in TBST buffer (10 mM Tris-HCl, pH 7.5, 100 mM NaCl, and 0.1% Tween 20) at 4°C and then incubated at room temperature (RT) with the anti-α4 antibody diluted 1:5000 (0.04 μg/ml) in the same blocking buffer for 1 hr, washed with TBST, and incubated with a peroxidase-conjugated rabbit anti-sheep antibody (Cappel, West Chester, PA) diluted 1:5000 (9.9 μg/ml) for 1 hr, after which membranes were washed again. Bound peroxidase was detected using enhanced chemiluminescence (ECL; Amersham). As a control, an identical gel was run in parallel with the anti-α4 antibody preadsorbed at 37°C with a 10-fold molar excess (2 μg/ml) of the synthetic peptide (Santa Cruz Biotechnology) for 3–4 hr. No immunostaining was observed under these circumstances.

Western blot and immunohistochemistry in human embryonic kidney cells transfected with nicotinic receptor subunit cDNAs. Human embryonic kidney (HEK-293) cells were transfected with cDNAs corresponding either to the rat α3, α4, and β4, or the human α4 and β2, or (for control purposes) the chimeric α7-V201–5HT$_3$ receptor (Eiselé et al., 1993) by the calcium phosphate DNA precipitation method as previously described (Chen and Okayama, 1987).

The level of expression of nicotinic receptors in this transient system was assessed by an equilibrium binding assay. Briefly, cells were harvested as previously described (Corringer et al., 1995) and incubated for 30 min at RT with [^{3}H]epibatidine (0.4 nM), in the absence or presence of 0.5 mM unlabeled nicotine to measure nonspecific binding. The level of expression was typically 0.2 pmol of binding sites per confluent 10 cm dish. The cell membrane fraction was obtained for subsequent use in Western blot analysis.

Cells were recovered and homogenized using an antiprotease buffer [0.1 M PBS, pH 7.4, 50 mM EDTA, and 0.5 mM phenylmethylsulfonyl fluoride (PMSF)]. Pellets were resuspended after centrifugation at 600 × *g* for 10 min in cold buffer (50 mM Tris–acetate, pH 7.4, 50 mM EDTA, 0.5 mM PMSF, and 0.2 U/μl aprotinine). DNA was eliminated by centrifugation at 400 × *g* for 10 min. Supernatants were centrifuged at 12,000 × *g* for 1 hr to pellet the membranes. Forty microgram aliquots were run in SDS-PAGE gels and developed as indicated above.

The immunohistochemical reaction was performed after fixation of cell cultures with 3% paraformaldehyde for 30 min at RT. After rinsing, free aldehyde radicals were neutralized in 50 mM NH_4Cl, 1 mM glycine, and 1 M lysine in 0.1 M PBS buffer, pH 7.4, for 20 min at RT. Cells were then blocked in PBS buffer containing 5% normal horse serum for 30 min and then incubated at 4°C with the anti-α4-subunit nAChR antibody (Santa Cruz Biotechnology) diluted 1:1000 (0.2 μg/ml) in PBS containing 1% normal horse serum overnight. After three 10 min washes in PBS, cells were incubated at RT with Cy3-conjugated anti-goat IgG (Amersham, Pittsburgh, PA) diluted 1:500 (2 μg/ml). Controls for method specificity consisted in omission of the primary antibody. The use of nontransfected cells and of α7-V201–5HT$_3$ (Eiselé et al., 1993) transfected cells in the same conditions yielded no immunostaining. For the peptide competition control, the primary antibody was preincubated at 37°C with 2 μg/ml of the synthetic peptide used for immunization for 3–4 hr. No immunostaining was observed under these circumstances.

Light microscope immunohistochemistry. Fifteen adult (200–250 gm) Sprague Dawley rats (*R. norvegicus*) of either sex were anesthetized with 35% chloral hydrate (0.1 ml/100 gm) and perfused through the ascending aorta with 200 ml of a 4% paraformaldehyde (freshly depolymerized) in 0.1 M PBS, pH 7.2, at RT. Brains were removed and post-fixed in the same fixative overnight at 4°C. After rinsing in abundant PBS, 50- to 60-μm-thick vibratome sections were collected in PBS and processed as free-floating sections at 4°C. Endogenous peroxidase activity was inhibited by pretreatment of the free-floating sections with 3% H_2O_2 in PBS for 15 min at RT. Nonspecific sites were blocked for at least 1 hr in PBS containing 4% bovine serum albumin (BSA) and 0.25% Triton X-100 at RT, rinsed three times for 10 min in PBS, and incubated overnight with the primary antibody anti-nAChR α4-subunit (Santa Cruz Biotechnology) diluted 1:1000 (0.2 μg/ml) in blocking buffer, at 4°C. After three 10 min rinses in PBS, sections were incubated in biotinylated rabbit anti-goat antibody (Amersham) diluted 1:200 (6.5 μg/ml) in blocking buffer at RT for 1 hr, rinsed again, and incubated in the avidin–biotin–peroxidase complex (ABC kit; Vectastain; Vector Laboratories, Burlingame, CA), all of them at RT. Bound peroxidase was revealed using 0.05% diaminobenzidine tetrahydrochloride (DAB; Sigma, St Louis, MO) and 0.01% H_2O_2 in PBS, at RT. Sections were mounted on gelatinized slides, dehydrated in a graded series of ethanols, and coverslipped with Eukitt mounting medium.

Method specificity was controlled either by omitting the primary antibody or by its preadsorption with the immunogenic peptide. For the peptide competition control, the primary antibody was preincubated at 37°C with 2 μg/ml of the peptide for 3–4 hr. No immunostaining could be observed in either case.

Double immunostaining for confocal microscopy. Free-floating vibratome sections (50 μm) from six rats [bregma levels, −5.20 to −5.80 mm, according to Paxinos and Watson (1986)] were pretreated in blocking buffer (4% BSA and 0.25% Triton X-100 in PBS) at RT for 1 hr and then incubated with two different primary antibodies: the anti-α4-subunit nAChR (Santa Cruz Biotechnology) used at 1:1000 dilution (0.2 μg/ml)

Table 1. Triplicate quantification of immunopositive (+) and unlabeled (−) neurons after double-labeling of the α4-subunit and TH by confocal microscopy (first column) in the rat SNpc

	Experiment 1	Experiment 2	Experiment 3	Mean ± SEM
α4(+)TH(+)	91.4% (341)	92.7% (318)	94.2% (163)	92 ± 0.3%
α4(+)TH(−)	6.7% (25)	4.9% (17)	2.3% (4)	5.8 ± 0.4%
α4(−)TH(+)	1.8% (7)	2.3% (8)	3.4% (6)	2 ± 0.1%

Percentages of neurons double- and single-labeled using antibodies against α4-subunit and TH are indicated for each separate experiment, with numbers of neurons sampled between brackets.

and a monoclonal antibody to TH (MAB318; Chemicon, Temecula, CA) at a 1:500 dilution (4 μg/ml). Two different protocols were used with identical results.

In the first one, both antibodies were diluted together in the blocking buffer, the incubation proceeded at 4°C overnight. After washing, all of the following steps were performed in the dark and at RT. Sections were incubated with a mixture of biotinylated rabbit anti-goat IgG (Jackson ImmunoResearch, West Grove, PA) diluted 1:200 (6.5 μg/ml) and Cy5-conjugated anti-mouse IgG (Amersham, Arlington Heights, IL) diluted 1:600 (1.6 μg/ml) in blocking buffer for 1 hr. Sections were then washed in PBS and incubated with Cy2-conjugated streptavidin (Amersham) diluted 1:600 (1.6 μg/ml) in blocking buffer for 1 hr.

In the second protocol, immunostaining for the two primary antibodies was developed sequentially. The sections were incubated first with the goat polyclonal antibody to α4-subunit followed by incubations in biotinylated anti-goat IgG (Jackson Immunoresearch) and then in Cy2-conjugated streptavidin (Amersham). After three 10 min rinses in PBS the sections were incubated in the monoclonal anti-TH antibody followed by Cy5-conjugated anti-mouse IgG (Amersham, Arlington Heights, IL). After rinsing in PBS, the sections were mounted, coverslipped with a 1:1 solution of PBS and glycerol, and examined in a Leica TCS NT confocal laser-scanning microscope equipped with an argon/krypton-mixed gas laser with excitation peaks at 488 nm (for Cy2) and 647 nm (for Cy5). Confocal image series were recorded through separate channels for the fluorescence of Cy2 and Cy5.

Immunofluorescently stained neurons were quantified on three rats (Table 1) by collecting images from a total of 26 distinct fields, each representing 329 × 329 × 35 μm of SNpc tissue.

Electron microscope pre-embedding immunoperoxidase. Vibratome sections from nine rats were used for electron microscopy. They were cryoprotected in sucrose–glycerol–PBS mixtures before being submitted to several freeze–thaw cycles in liquid nitrogen. This membrane permeabilization treatment was preferred to exposure to Triton X-100 because it was less detrimental to ultrastructural morphology. Vibratome sections were then rinsed in large volumes of PBS, blocked and incubated overnight at RT in primary antiserum, and then processed as above for peroxidase. Addition of 0.1% glutaraldehyde did not modify the pattern of immunolocalization. Once the peroxidase activity was detected, sections were post-fixed in OsO_4 dehydrated in a graded series of ethanol, propylene oxide, and flat embedded in epoxy resin (Durcupan ACM). Coronal sections of the mesencephalon were examined with the light microscope and drawn using a camera lucida. The region of SNpc corresponding to bregma −5.80 mm, ventral 8.4 mm, and 1.3 mm from the midsaggital plane (Paxinos and Watson, 1986) was one of the richest in α4-subunit-LI positive neurons. This medial part of the SNpc was selected because it is also densely populated with DA neurons and axonal branches containing ACh (Fallon and Loughlin, 1995) and choline acetyltransferase (ChAT; Henderson and Sherriff, 1991) immunoreactivity. It is also the zone in which Futami el al. (1995) found synaptic nicotinic transmission. Samples were cut out from the slides and glued to blank blocks of resin. Ultrathin sections were cut and examined, without any further contrasting, with a Philips CM10 electron microscope (EM) at 60 kV.

The method specificity was controlled either by omitting the primary antibody or by preabsorption with the antigenic peptide. No immunoperoxidase labeling was observed with either of these controls.

Electron microscope postembedding immunogold labeling. For immunogold labeling, several combinations of fixative were tested: 4% formaldehyde (freshly depolymerized from paraformaldehyde) applied according to a "pH shift protocol" (Nagelhus et al., 1998), 4% formaldehyde plus 0.1% glutaraldehyde, or 4% formaldehyde plus 0.5% glutaraldehyde. The best immunogold labeling was obtained with the first two of these fixatives. Blocks of substantia nigra from two "pH-shift" rats, and from one "0.1% glutaraldehyde" rat were dissected out from vibratome sections, 400 μm in thickness, at the same stereotaxic levels as indicated above.

Embedding of tissue in Lowicryl HM20 resin was performed as described in Matsubara et al. (1996). Ultrathin sections, 90 nm, were etched for 1–3 sec in sodium ethanolate. Remnant aldehyde residues were neutralized by a 10 min treatment in 0.1% sodium borohydride plus 50 mM glycine in Tris-buffered saline plus 0.1% Triton X-100 (TBST) for 10 min. Grids were then incubated for 10 min in a blocking solution of TBST and 2% human serum albumin to block the nonspecific binding sites.

Different concentrations of NaCl ranging from 0.3 to 0.9% were tested. The best immunolabeling was obtained with 0.5–0.6% NaCl in the vehicle buffer, and when the grids were incubated at RT successively in the blocking solution for 120 min, first antibody (goat polyclonal IgG anti-α4 from Santa Cruz Biotechnology) 1:1000 (0.2 μg/ml), followed by washes in TBST, and 60 min incubation in an immunogold reagent 1:40 (IgG rabbit anti-goat 10 nm gold-conjugate; Aurion) in the same blocking solution plus 0.5% polyethylene glycol (20,000 molecular weight).

For controls, as in the immunoperoxidase protocol, the method specificity was examined either by omitting the primary antibody or by preabsorption with the antigenic peptide. No immunogold labeling was observed when the first antibody was omitted. When using preadsorbed primary antibodies, some gold particles were present mainly in the somatodendritic cytoplasm, and very few were found on plasma membranes of extrasynaptic and postsynaptic domains of the neuronal cell surface.

After washes, the ultrathin sections were dried, stained with 1% uranyl acetate and 0.3% lead citrate, dried, and observed in a Philips CM10 EM at 80 kV. Magnification was calibrated with a cross grating replica.

RESULTS

Specificity of the immunohistochemistry

The anti-α4-subunit antibody used in this study is a peptide-purified polyclonal antibody that recognizes an intracellular epitope in the α4-subunit protein. The specificity of this polyclonal antibody was tested using several methods.

First, in Western blots, the anti-α4-subunit antibody reacted with a single band present in rat brain homogenates and absent in lung homogenates. This specific band had an apparent molecular weight of ~70 kDa, which corresponds to the approximate range where immunopurified α4-subunit protein is found (Whiting et al., 1987). Preadsorption with the corresponding synthetic peptide used for immunization led to a dramatic diminution in the labeling intensity of this band (Fig. 1).

Second, SDS solubilized membranes from HEK-293 cells transfected with rat cDNAs corresponding to the α4β4 and α3β4 subunits, α7–$5HT_3$ construct, the α4β2 human subunit cDNAs, and nontransfected cells were used in immunoblots studies. We detected one band in the expected molecular weight range, 70 kDa, in the membranes from cells that had been transfected with either α4β4 rat cDNAs or α4β2 human cDNAs, but this band was not present in either α3β4, α7–$5HT_3$-transfected, or in nontransfected cell extracts (Fig. 2).

When the immunofluorescence technique was used directly in transfected HEK-293 cells, an immunopositive reaction was present in association with membranes of cells that had been

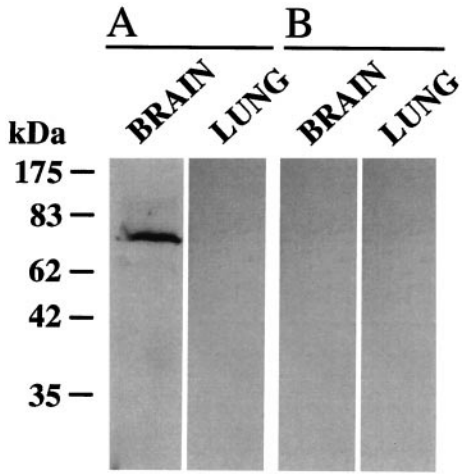

Figure 1. Analysis of the α4-subunit antibody specificity by immunoblot of total homogenates of rat brain and lung. Equivalent amounts of protein from each fraction (50 μg) were subjected to SDS-PAGE, transferred to nitrocellulose, and probed with the polyclonal antibody against the α4-subunit of the nAChR. *A*, After incubation with the anti-α4-subunit antibody, one specific band was positive in brain homogenates and was not present in lung homogenates. *B*, Incubation with the α4-subunit antibody pre-adsorbed with the corresponding synthetic peptide used for immunization has led to a dramatic diminution in the labeling intensity of this band in brain homogenates.

transfected with either α4β4 rat cDNA or α4β2 human cDNA (Fig. 3) but not in nontransfected cells.

Additional evidence for specificity of the antibody used in the present study comes also from Western blot analysis using homogenates of brains of mice lacking the α4-subunit (Marubio et al., 1999), which shows the disappearance of the 70 kDa band corresponding to the α4-subunit.

Having demonstrated its specificity by Western blot analysis, we then used the anti-α4 antibody in an immunohistochemical study of the expression of α4-subunit protein in the adult rat brain. Method specificity was studied by omitting the primary antibody as well as by incubation in the presence of an excess of the synthetic peptide. No cellular labeling was apparent under either of these conditions (data not shown).

Altogether these data strongly support the specificity of this antibody in tissue sections. The α4-subunit-LI pattern thus suggests the localization of the α4-subunit.

Immunohistochemical localization in rat brain

Incubation of tissue sections with the anti-α4 antiserum generated reproducible patterns of staining within discrete populations of neurons and neuronal processes. The sensitivity of the immunohistochemical procedure was sufficient for strong labeling of cells of the SNpc complex (Fig. 4*A*) and reliable staining in other brain areas shown by ISH to express α4 mRNA, such as the cerebral cortex (Fig. 5*A*), the globus pallidus (Fig. 5*B*), and some nuclei of the thalamus. In general, the pattern of immunolabeling was in good agreement with the pattern detected earlier by ISH (Wada et al., 1989).

The immunohistochemical reaction was restricted to neurons and was present in cell perikarya and dendrites but absent from cell nuclei (Fig. 4*B*). In the mesencephalon, immunoreactivity for the α4-subunit was more intense in nuclei containing dopaminergic cells than in other groups of neurons. α4-subunit-LI neurons were present mainly in the SNpc and in the VTA, but some of them were also detected in the predominantly nondopaminergic reticular portion of the substantia nigra (SNpr) (Fig. 4*A*). No evidence for staining of axon terminals in the caudate putamen and the nucleus accumbens, the terminal projection area of the dopaminergic neurons in the midbrain, was observed (Fig. 5*B*). A few somata in the caudate putamen, however, were found immunoreactive for the α4-subunit.

Colocalization studies

Given the high level of expression of α4-subunit mRNA and -LI in the dopaminergic cell groups and the importance of these nuclei in the central actions of nicotine, we directly tested whether the α4-subunit expressing neurons in the midbrain were dopaminergic. The transmitter identity of the α4-subunit-LI positive neurons was examined by double-labeling sections of the rat midbrain for both the α4-subunit-LI and TH, the rate-limiting enzyme responsible for the synthesis of DA. A quantitative estimation of double- or single-labeled neurons in SNpc revealed that 92% of neurons were double-labeled for the α4-subunit-LI and TH (Table 1). Thus, the majority of cells immunoreactive for TH were found to be labeled by the antibody against α4 (Fig. 6); conversely, only 5.8% of neurons immunoreactive for the α4-subunit did not coexpress TH. The identity of the neurotransmitter of these cells remains to be determined. Moreover, the intensity of its α4-subunit immunostaining was weak as compared with that of double-stained neurons. Thus, a strong correlation exists between the dopaminergic status of the neuron and the expression of the α4-subunit-LI. These results are in agreement with recent colocalization studies done in SNpc using a different antibody against nAChRs α4-subunit (Sorenson et al., 1998). Double labeling of cells with antibodies against α4-subunit and glial fibrillary acidic protein showed no localization of the α4-subunit-LI in glial cells (data not shown).

Ultrastructural localization of α4-subunit-LI in the SNpc

The subcellular localization of the α4-subunit-LI was initially examined by a pre-embedding immunoperoxidase method. Electron microscopy observations confirmed that in the SNpc, the α4-subunit-LI reaction was found associated with neurons. For illustration (Figs. 7, 8), we selected neurons in which the reaction product was not so massive that cytoplasmic compartments were

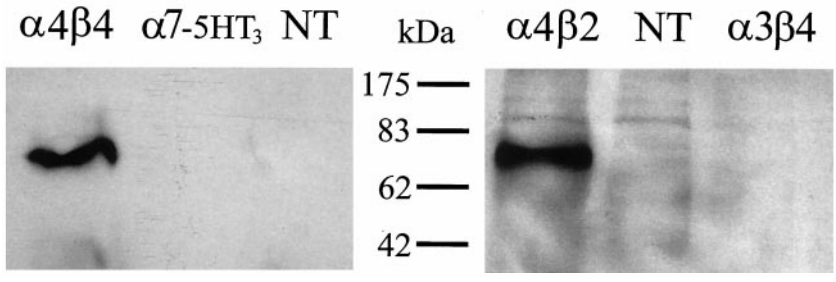

Figure 2. Immunoblot analysis of the α4-subunit antibody specificity in membranes extracted from HEK-293 cells transfected with different cDNAs of nAChRs. We detected one band of the expected molecular weight range only in the cells that were transfected with either α4β4 rat cDNAs (*left*) or α4β2 human cDNAs (*right*). This band was not present in either α3β4 rat cDNAs, in α7–$5HT_3$-transfected, or in nontransfected cell extracts (*NT*).

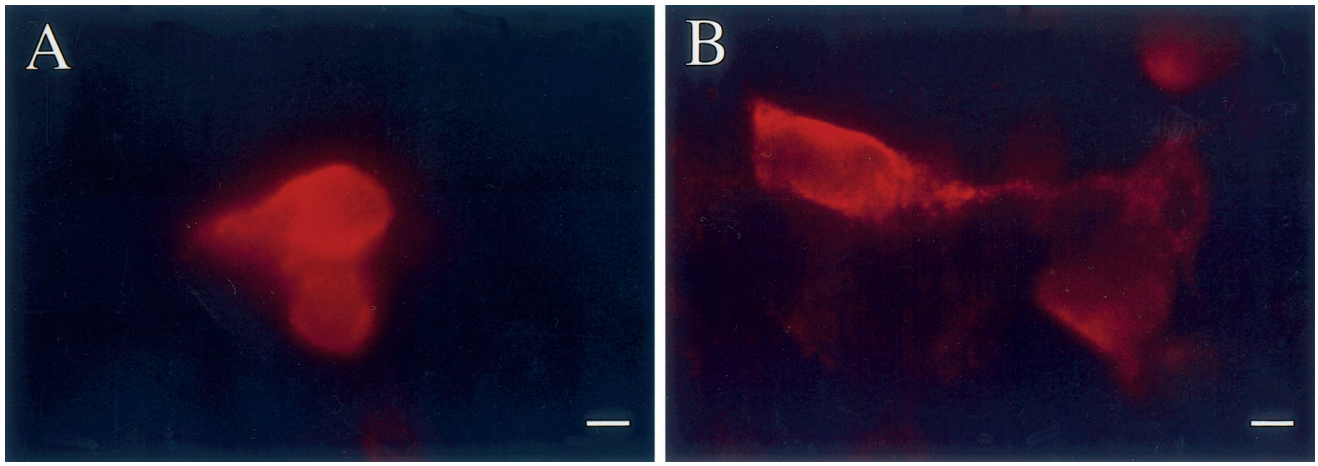

Figure 3. Staining of transfected HEK-293 cells with the α4-subunit antibody. Immunofluorescence positive signal was present in HEK-293 cells transfected with either (*A*) α4β2 human cDNAs or (*B*) α4β4 rat cDNAs. Scale bar, 10 μm.

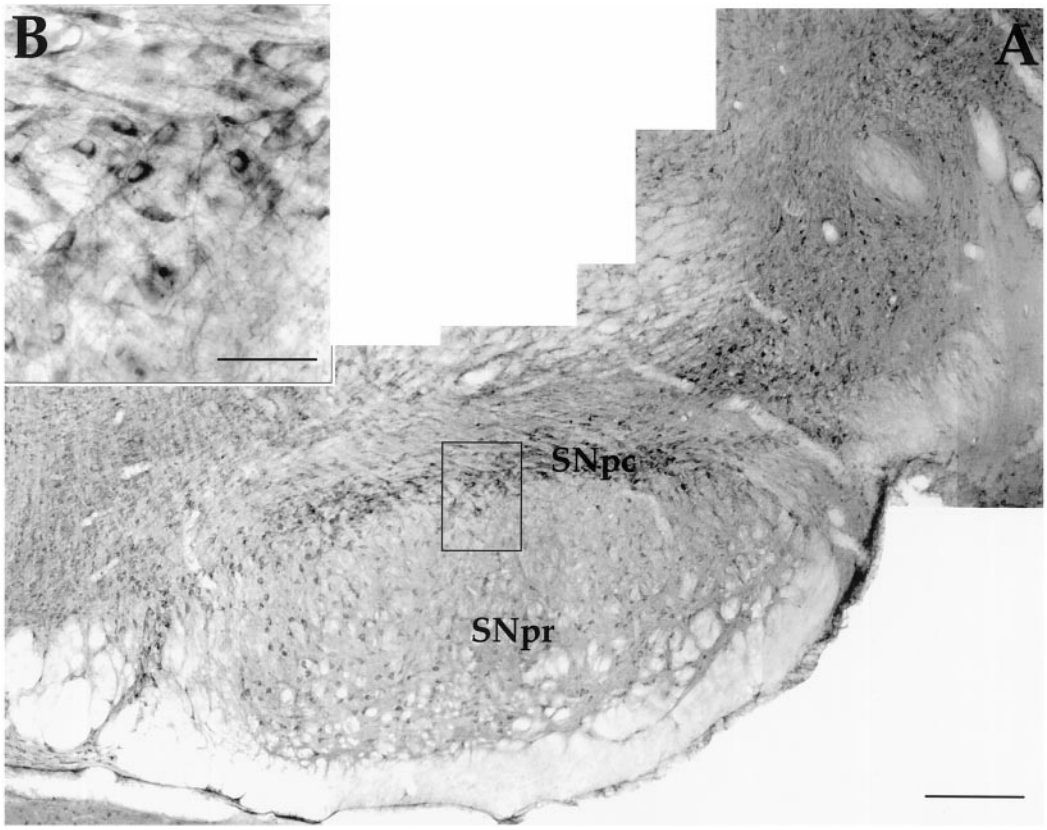

Figure 4. Distribution of nAChR α4-subunit-LI neurons in the adult rat substantia nigra. *A*, Coronal sections containing rat SNpc and SNpr were stained with the α4-subunit antibody detected using immunoperoxidase method. Scale bar, 200 μm. *B*, The α4-subunit-LI was present in neuronal perikarya and dendrites, but absent from cell nuclei as shown in this detail of SNpc-immunopositive cells. Scale bar, 50 μm.

obscured. In these cells, the α4-subunit-LI reaction product was localized in perikarya and dendrites. It appeared as clumps of dense material associated with the rough endoplasmic reticulum (RER) and the cytoplasmic matrix (Fig. 7*A*). No immunostaining was observed with preadsorbed antibody or in the absence of the first antibody in the pre-embedding immunoperoxidase procedure (Fig. 8*D*), as well as in the postembedding immunogold procedure (Fig. 9*H*). As in previous work with the β2-subunit (Hill et al., 1993), we never observed α4-subunit-LI reaction in the Golgi apparatus (Fig. 7*B*). In the perikarya, the α4-subunit-LI reaction was distributed in a more patchy manner (Fig. 7*A,B*) than the β2-subunit-LI reaction product (Hill et al., 1993). The α4-subunit-LI DAB reaction product was found associated with microtubules in dendrites (Fig. 8*B,C*). Dense accumulations of α4-subunit-LI reaction product were also observed associated with a few asymmetrical synaptic profiles located on both perikarya (Fig. 8*A*) and dendritic shafts (Fig. 8*B*), but never on dendritic spines. These observations suggest that α4-subunit-LI

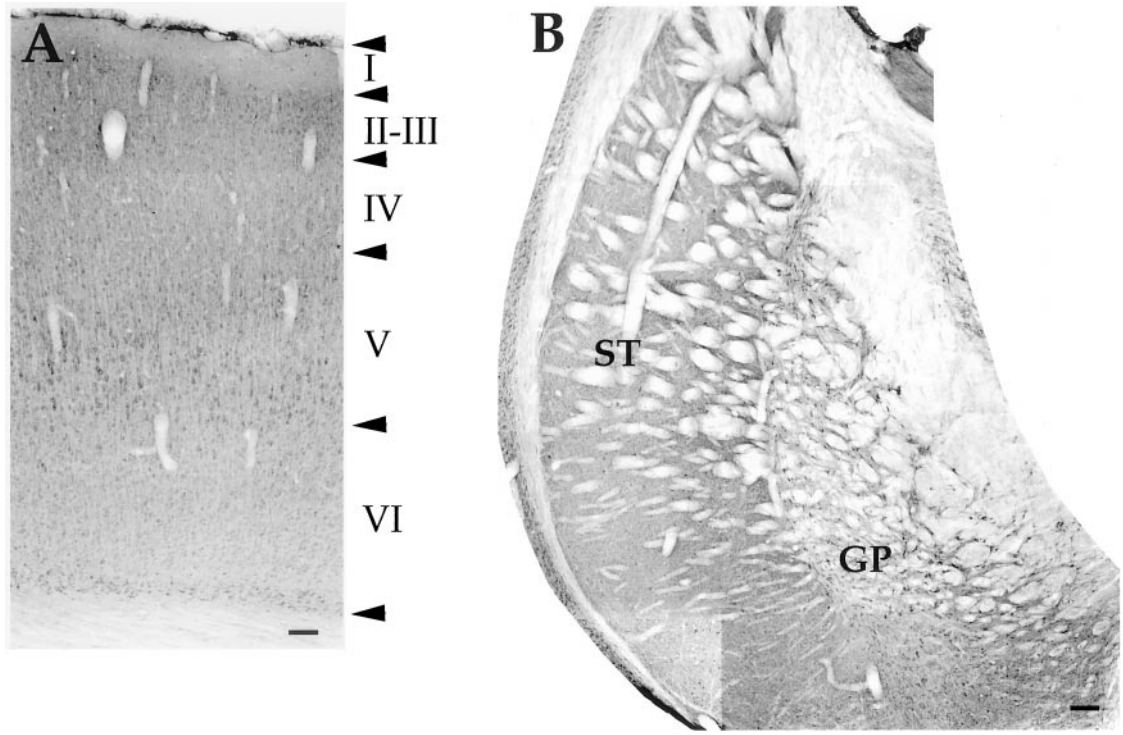

Figure 5. Distribution of α4-subunit-LI in cerebral cortex, globus pallidus (*GP*), and striatum (*ST*) after immunoperoxidase labeling. *A*, Coronal sections of rat somatosensory cortex show a laminar distribution of α4-subunit-LI, mainly in neurons of the infragranular layers. Cell bodies and apical dendrites of pyramidal neurons show a prominent labeling. Scale bar, 100 μm. *B*, Cell bodies of globus pallidus were clearly stained with α4-subunit antibody but few neurons were positive in the striatum. Scale bar, 100 μm.

positive synaptic profiles are preferentially located on the perikarya and proximal dendrites of the neurons in the SNpc. Large deposits of DAB immunoreaction product could not be detected (Fig. 8*A–C*) in the perisynaptic, i.e., around the edge of postsynaptic density (unlike as in Luján et al., 1996, their Fig. 6) domains of the neuronal cell surface. The frequency of the DAB-decorated postsynaptic densities was low.

Because DAB precipitates may be deposited at some distance from the epitopes, we attempted to confirm a possible synaptic localization of the α4-subunit by postembedding immunogold experiments, which provides a better resolution. As shown in Figure 9*A–G*, gold particles were observed associated with some postsynaptic densities. The scarcity of the observations of gold-decorated postsynaptic densities paralleled that of DAB-positive synaptic profiles. Although the resolution of the postembedding immunogold labeling of single sections is high, it will necessarily give a lower proportion of immunopositive synapses than pre-embedding peroxidase labeling because only the epitopes exposed at the surface of the ultrathin sections will be accessible to the immunoreagents (Griffiths, 1993). Only a small proportion of the receptor-bearing synapses will be recognized as such. Accordingly, we found fewer immunolabeled synapses with the immunogold labeling. From an estimated 60,000 synapses observed directly on the EM screen, we found 102 synaptic profiles decorated with at least one gold particle (Fig. 10*A*). The distribution of gold particles per profile did not follow a Poisson distribution (Fig. 10*B*) for synaptic profiles with two, and more, gold particles per profile, suggesting that a threshold of two gold particles per profile should be used to consider it as labeled. Thus, only 63 of the synaptic profiles could be considered as labeled. Of these, only 44 were decorated with gold particles located within 30 nm distance from the postsynaptic plasma membrane (Fig. 11), which is the criterion defined by Matsubara et al. (1996). Finally, only 31 of the narrowed group of synaptic profiles showed distinct appositions of presynaptic and postsynaptic plasma membranes, a synaptic cleft 10–20 nm wide, and the presence of synaptic vesicles in the nerve terminals (Peters et al., 1991). This selected population contained 114 gold particles with a mean of 3.6 ± 3.1 (mean ± SD; $n = 31$) gold particles per synaptic profile. The mean of the density of gold particles calculated for each of these 31 synaptic profiles is 10.7 ± 11.6 ($n = 31$) gold particles per micrometer of decorated postsynaptic plasma membrane (total measured length of 14.2 μm). The estimated mean length of postsynaptic plasma membranes was 0.49 ± 0.27 μm ($n = 114$), giving 38.8×10^{-4} gold particles per micrometer of total postsynaptic plasma membrane (total length of 60,000 × 0.49 μm). The background was estimated after immunolabeling with antibody preadsorbed with the immunogenic peptide. We scanned the same number of synaptic profiles as in the experimental sample ($n = 60{,}000$). We found seven profiles decorated with at least one gold particle (Fig. 10*A*). After the same criteria used for the experimental sample, only one profile decorated with two gold particles was observed, giving 0.68×10^{-4} gold particles per micrometer of total postsynaptic plasma membrane (total length of 60,000 × 0.49 μm).

On the extrasynaptic plasma membrane of the dendrites we found a density of 0.10 ± 0.15 ($n = 27$) gold particles per micrometer (total length sampled, 316 μm), and the background was 0.01 ± 0.04 ($n = 31$) gold particles per micrometer (total length sampled, 185 μm). Evidence thus exists that the α4-subunit is localized at authentic, albeit very scarce, postsynaptic membranes in DA neurons.

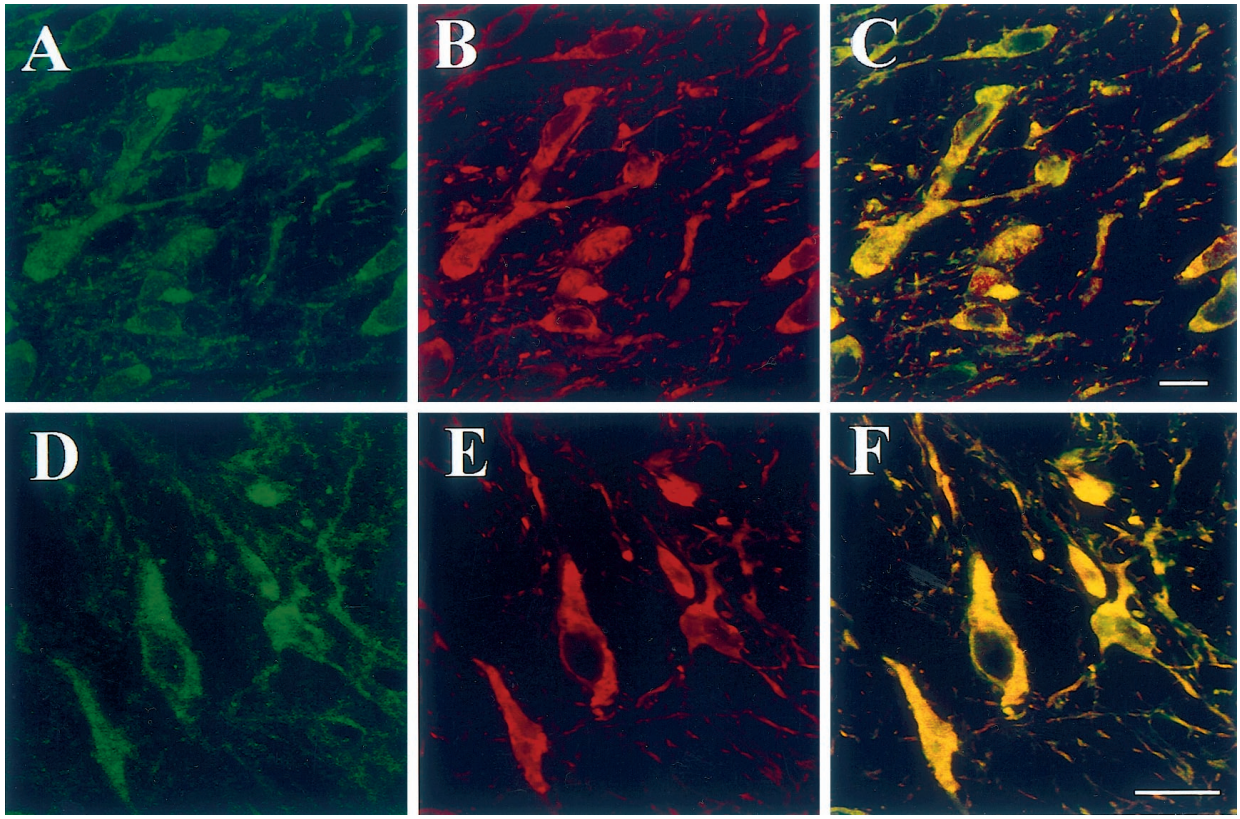

Figure 6. Confocal microscopy shows colocalization of α4-subunit-LI and TH in dopaminergic neurons in the SNpc (*A–C*) and VTA (*D–F*). *A*, *D*, Cy2-conjugated streptavidin decorates neurons immunolabeled with the antibody raised against the α4-subunit. *B*, *E*, Cy5-conjugated anti-mouse IgG-stained neurons containing TH. Superimposition of the images (*C*, *F*) show that most of the neurons were double-labeled. Scale bar, 20 μm.

DISCUSSION

Together with the β2-subunit, the α4-subunit of the nAChR is one of the most widely expressed nAChR subunits in the CNS. Using an antibody specific for the α4-subunit we have shown a widespread distribution of this subunit in the rat brain. The expression of the α4-subunit was particularly intense in DA neurons of the SNpc and VTA where α4-subunit-LI colocalizes with TH. Furthermore, α4-subunit-LI was found in association with some postsynaptic densities in the DA neurons.

Specificity of α4-subunit immunostaining

The α4-subunit immunolabeling was found to be highly specific both in tissue homogenates and sections of rat brain. Such specificity was further confirmed using mice lacking the α4-subunit (Marubio et al., 1999). Western blot analysis using the anti-α4-subunit antibody showed the disappearance of a band corresponding to 70 kDa in brain extracts from these mice lacking the α4-subunit, although it is still present in control mice (Marubio et al., 1999). There was a good correspondence between areas where neurons exhibited a dense cytoplasmic α4-subunit-LI staining and regions where a positive ISH signal was observed using probes for the α4-subunit mRNA (SNpc–VTA, thalamus, and cortex) (Wada et al., 1989).

The regional distribution of α4-subunit-LI differs unambiguously from that of other nAChR subunits. For instance, the α2-subunit that has the highest peptide sequence similarity to the α4-subunit of the known nAChR is present in high mRNA levels in the interpeduncular nucleus (Wada et al., 1989). However, α4-subunit mRNA levels are lower, and α4-subunit-LI cannot be detected in this area.

The β2-subunit of the nAChR is present in most neurons of the rat brain, as shown by both ISH (Wada et al., 1989) and immunohistochemistry techniques (Swanson et al., 1987; Hill et al., 1993). The α4-subunit-LI pattern differs from that of β2-subunit-LI especially in the striatum and hippocampus, where only a few positive α4-subunit-LI cells were detected. Moreover, the α4-subunit-LI continues to be expressed in unaltered levels (data not shown) in mice lacking the β2-subunit of the nAChR (Picciotto et al., 1995) indicating that this antibody does not cross-react with the β2-subunit.

The pattern of the α4-subunit-LI in general parallels the pattern of high-affinity [^{3}H]nicotine binding sites in the rat brain (Clarke et al., 1985b). There is moderate to strong labeling in the medial habenula, thalamus, SNpc, and VTA, and weaker labeling in the hippocampus. Furthermore, the pattern of the α4-subunit-LI does not match the pattern of ^{125}I-α-bungarotoxin (α-BTX) binding sites, which reflects the distribution of the α7-subunit (Seguela et al., 1993; Orr-Urtreger et al., 1997). The distribution of ^{125}I-α-BTX labeling is strong in the hippocampus and weak in the superficial cortical layers, whereas α4-subunit-LI is strong in the cortex and weak in hippocampus. At the level of the hypothalamus α4-subunit-LI is present but the densities of high-affinity [^{3}H]nicotine binding sites or α4 mRNA are rather low (Clarke et al., 1985b; Wada et al., 1989). In the striatum, we found some neurons with α4-subunit-LI, although mRNA have not been reported in this structure (Wada et al., 1989). Differ-

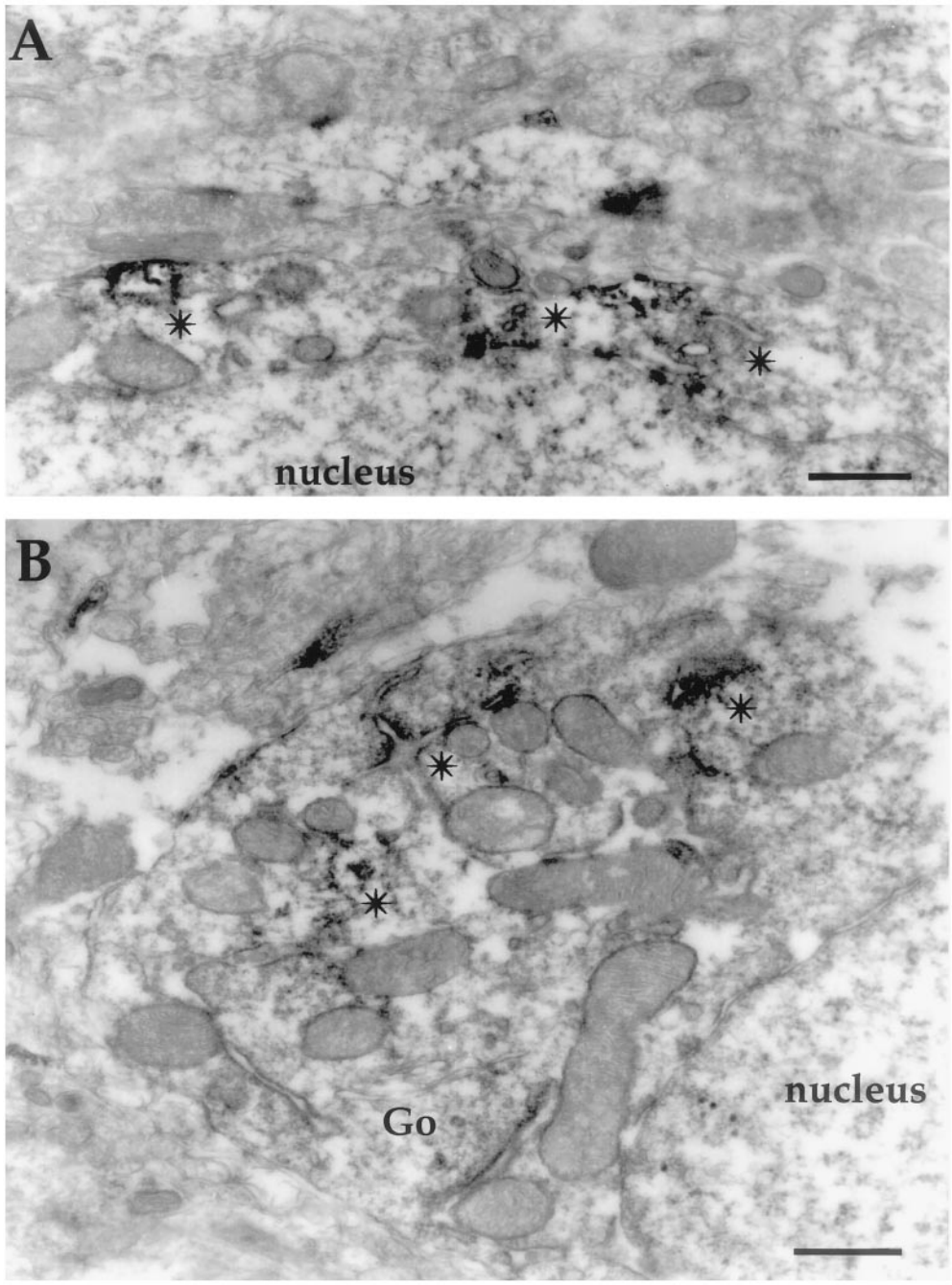

Figure 7. Ultrastructural localization of the α4-subunit of the nAChR in the rat SNpc, using immunoperoxidase labeling. *A*, Dense deposits of DAB are observed in spots of the somatodendritic compartments (*asterisks*). *B*, Immunoreactivity for the α4-subunit is distributed heterogeneously. In the perikarya, immunolabeling is frequently associated with endoplasmic reticulum (*asterisk*), but not with the Golgi apparatus (*Go*). Scale bar, 0.4 μm.

ences in the distribution of nAChRs and their mRNAs at the cellular level may result either from higher sensitivity of immunocytochemical techniques as compared with ISH, or from higher translational efficiencies.

The α4-subunit in dopaminergic neurons of the SNpc and VTA

The composition of the nAChRs that mediate the effect of nicotine on DA neurons is only partially known. Recent results have shown that the response of SNpc and VTA neurons to nicotine is absent in mice lacking the β2-containing receptors (Picciotto et al., 1998). This suggests that the β2-subunit is an integral part of the nAChRs that mediates nicotine-elicited responses on DA neurons.

It remains to be determined which other nicotinic subunits assemble with the β2-subunit in DA neurons. Moderate to high levels of the α3, α4, α5, α6, β2, β3 nAChR-subunit mRNAs are present in these neurons (Wada et al., 1989, 1990; Deneris et al., 1989; Dineley-Miller and Patrick, 1992; Le Novère et al., 1996). The α6-subunit immunoreactivity was found to be present in DA neurons of the midbrain (Goldner et al., 1997). In addition, an α7-containing nAChR has been demonstrated with electrophysiological techniques (Pidoplichko et al., 1997).

Our present results, along with those from Sorenson et al. (1998), suggest that the α4-subunit protein is highly concentrated in DA cell bodies and proximal dendrites. This is in line with previous work showing that a nAChR with a putative composi-

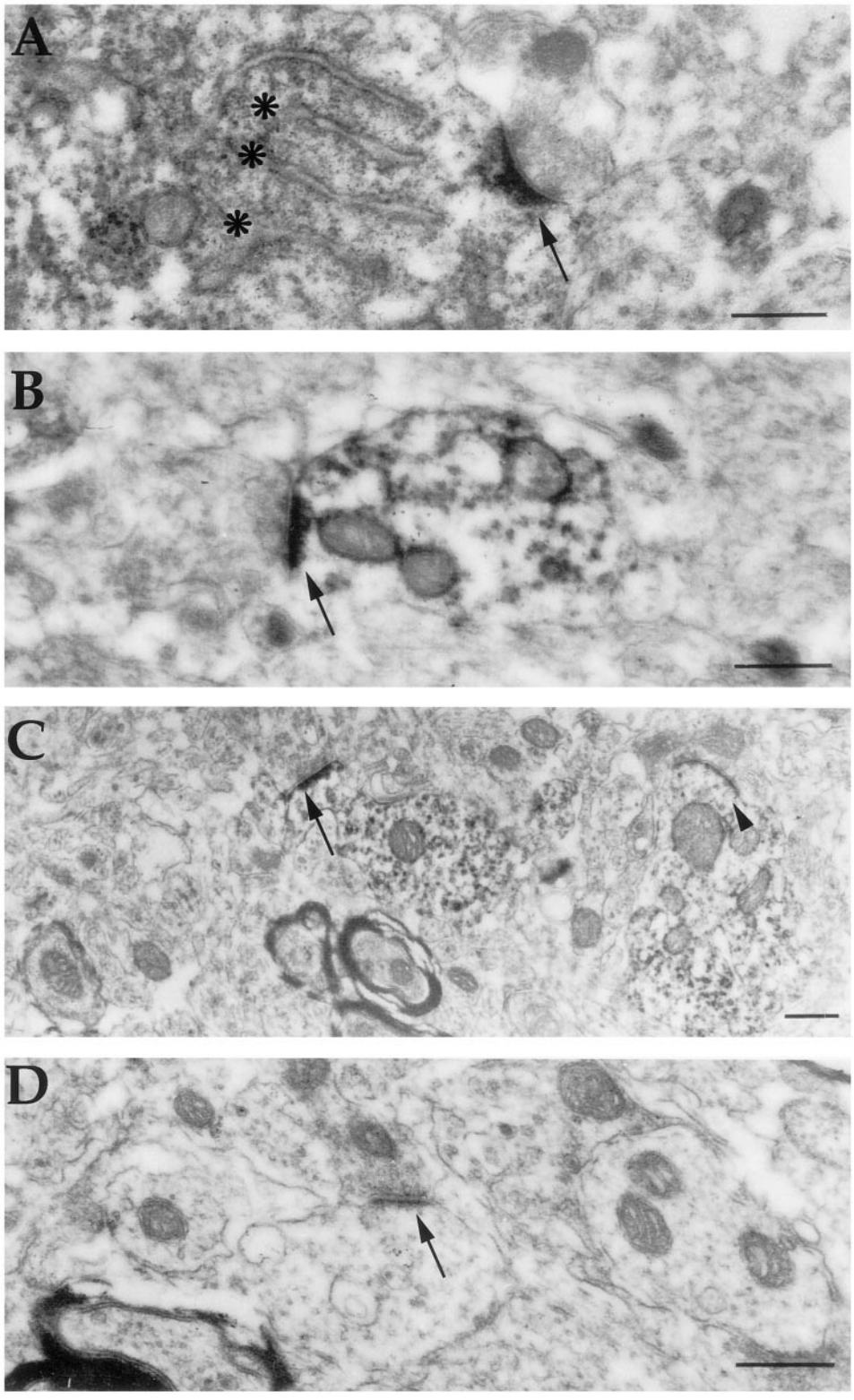

Figure 8. Postsynaptic localization of the α4-subunit-LI in the rat SNpc (*A–C*). Dense deposits of immunoreaction product are associated with postsynaptic densities (*arrows*) and not with perisynaptic plasma membrane. *A*, Densely immunolabeled axosomatic synaptic contact (*arrow*) is close to a lightly labeled endoplasmic reticulum (*asterisks*). *B*, Immunolabeled synaptic profile (*arrow*) on a dendritic shaft. Dendroplasm is also lightly immunolabeled. *C*, In the same field as in *B* and *C* unlabeled synaptic contacts (*arrowhead*) were present beside labeled synaptic profiles (*arrow*). *D*, No labeling was apparent in controls (*arrow*) in which the first antibody was either omitted or preadsorbed with the peptide used as antigen. Scale bar, 0.4 μm.

tion of α4β2 is responsible for nicotinic responses in mesencephalic DA cell bodies and disappears in β2 knock-out mice (Picciotto et al., 1998).

Indeed, different kinds of experiments have shown that high-affinity binding sites, which are enriched in the mesencephalic DA cell bodies, are most likely composed of α4β2-containing nAChRs (Whiting and Lindstrom, 1987; Flores et al., 1992; Happe et al., 1994; Zoli et al., 1998). It cannot be excluded that nicotinic transmission is mediated via α4/nonβ2 receptors in other brain regions (Zoli et al., 1998).

Taken together, the present and previous results suggest, but do not yet demonstrate, that the α4-subunit might be part of the nAChRs that contribute to the nicotinic activation of DA neurons in the mesotelencephalic pathways.

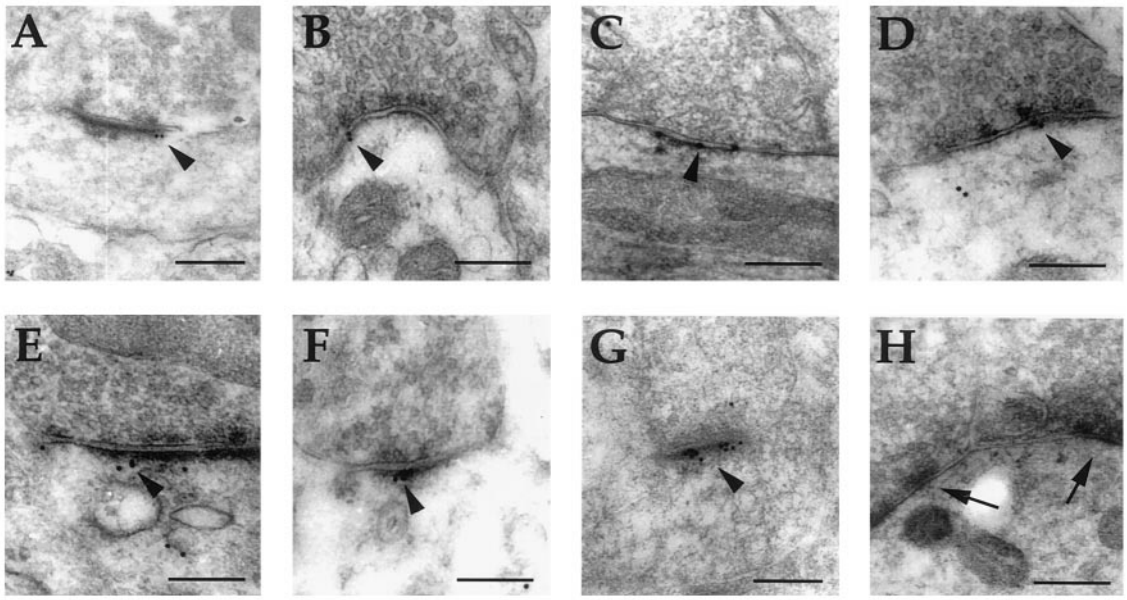

Figure 9. Postsynaptic localization of the α4-subunit-LI in the rat substantia nigra (*A–G*). Consistent with our observations using immunoperoxidase, the immunogold labeling is observed at some synaptic profiles (*arrowheads*). Most of the postsynaptic densities were decorated with two to four gold particles. To estimate the nonspecific labeling, the primary antibody was either omitted or preadsorbed with the antigen peptide before incubations. In that case, most of the synaptic profiles (*arrows*) were unlabeled (*H*). Scale bar, 0.25 μm.

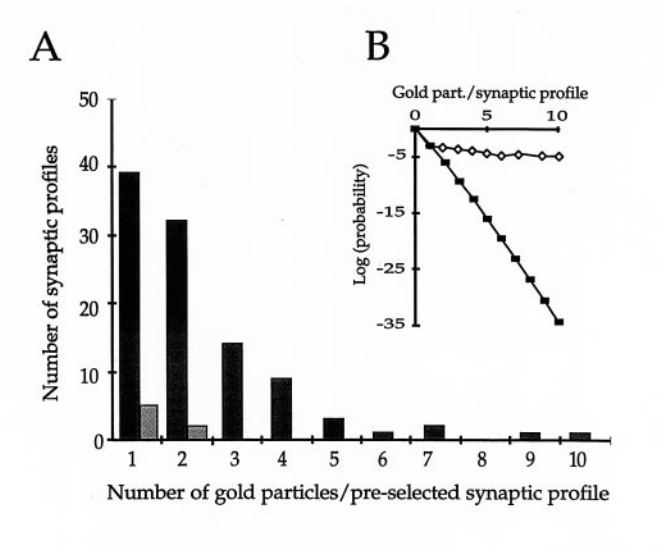

Figure 10. Histogram distribution of synaptic profiles decorated with one or more gold particles per profile (before applying the morphological and gold particle distribution criteria), in both experimental (*dark gray*) and control (*light gray*) conditions (*A*). In experimental conditions (*B*) this distribution (*open diamonds*) rapidly diverges from a Poisson distribution (*black diamonds*) for two and more gold particles per synaptic profile.

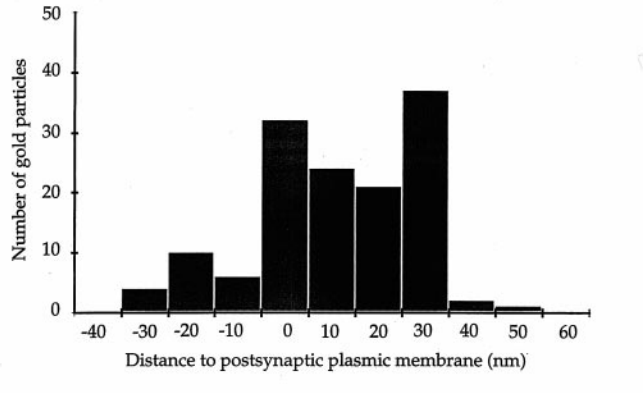

Figure 11. Histogram showing the radial distribution of gold particles over synaptic profiles sampled in the SNpc. The distances between the center of each gold particles and the postsynaptic plasma membrane were grouped into bins 10 nm wide. The values along the *x*-axis indicate bin centers, with bin "0" centered on the postsynaptic plasmic membrane. *Minus signs* indicate direction of the presynaptic domain. These data were pooled from 44 synaptic profiles.

The cholinergic circuits in the mesencephalic dopaminergic nuclei

Anatomical observations show that the mesencephalic DA nuclei receive a cholinergic innervation from the pedunculopontine tegmental nuclei (PPN) and the laterodorsal tegmental nucleus (Woolf and Butcher, 1986; Beninato and Spencer, 1987, 1988; Gould et al., 1989; Tokuno et al., 1988, but see Lee et al., 1988). High densities of muscarinic (Nastuk and Graybiel, 1991) and nicotinic receptors have been observed in the SNpc (see above), with a pattern resembling that of acetylcholinesterase (AChE) (Paxinos et al., 1980).

There is also functional evidence for cholinergic innervation (Clarke et al., 1987). For example, quinolinic acid lesions of the PPN attenuate the stimulatory effects of intranigral neostigmine, an AChE inhibitor, on DA efflux in the striatum, and intranigral nicotine enhances striatal DA efflux (Blaha and Winn, 1993; Blaha et al., 1996). Electrophysiological studies with slice preparations reveal nicotinic postsynaptic responses on DA neurons in the SNpc after stimulation of the PPN (Futami et al., 1995, but see Scarnati et al., 1986). These observations suggested that nicotinic receptors are involved in the pontonigral cholinergic transmission.

Ultrastructural studies demonstrated that ChAT-positive terminals form asymmetrical synapses with the cell bodies and dendrites of SNpc DA cells (Beninato and Spencer, 1987, 1988; Henderson and Greenfield, 1987; Martinez-Murillo et al., 1989a,b; Bolam et al., 1991; Henderson and Sherriff, 1991).

To date, few ultrastructural studies of nAChR localization have been performed in rat brain. Using two different monoclonal antibodies, mAb WF6 (raised against purified *Torpedo marmorata* electric organ) and mAb 299 (against chicken α4-subunit), α4-subunit-LI was found to be associated with some postsynaptic membranes in the cerebral cortex (Whiting and Lindstrom, 1988; Schroder et al., 1989; Okuda et al., 1993; Nakayama et al., 1995) and in dendrites of neurons from the SNpc of the rat (Sorenson et al., 1998). However, mAb WF6 competes for the α-BTX-binding site on *Torpedo* nAChRs and may recognize an α-BTX nAChR in brain.

We found α4-subunit-LI in perikarya and dendritic shafts of neurons in the substantia nigra and in association with some postsynaptic membranes. We also observed a strong staining of neuronal RER but failed to detect it over Golgi membranes. It is proposed that the α4-subunit-containing receptors accumulate in the RER in the course of biosynthesis and assemble, before being targeted to the neuronal cell surface.

Nonsynaptic transmission in this system cannot be excluded (Descarries et al., 1997). The α4-subunit might be localized extrasynaptically as was the case for other nAChRs subunits. For instance, in chick ciliary ganglion, immunohistochemical staining at the electron microscopy level indicated that α-BTX-sensitive receptors are localized in regions adjacent to postsynaptic membrane thickenings and are concentrated in the vicinity of short dendrites emanating from the cell bodies (Jacob and Berg, 1983). nAChRs that are recognized by mAb 35 (Tzartos et al., 1981) but not α-BTX can be found, in part, in the specialized postsynaptic membrane (Jacob et al., 1984; Loring and Zigmond, 1987). Similar conclusions were reached with confocal immunofluorescence that revealed clusters of α-BTX-binding nAChRs in perisynaptic locations (Horch and Sargent, 1995).

The synaptic profiles decorated with α4-subunit LI are quite rare, but their topological distribution, restricted to the perikarya and proximal dendrites of the DA neurons in the SNpc, might have a significant functional role that remains to be fully elucidated.

We suggest that the α4-subunit is part of functional nAChRs present on DA neurons. It seems likely to be involved in mediating the increase of dopamine release caused by nicotine. This mechanism may be relevant to brain reward circuits that plausibly could contribute to cognitive learning (Dehaene and Changeux, 1989, 1997; Levin et al., 1992, 1995) and nicotine addiction (Koob, 1996; Pontieri et al., 1996).

REFERENCES

Beninato M, Spencer RF (1987) A cholinergic projection to the rat substantia nigra from the pedunculopontine tegmental nucleus. Brain Res 412:169–174.

Beninato M, Spencer RF (1988) The cholinergic innervation of the rat substantia nigra: a light and electron microscopic immunohistochemical study. Exp Brain Res 72:178–184.

Bertrand D, Changeux JP (1995) Nicotinic receptor: an allosteric protein specialized for intercellular communication. Semin Neurosci 7:75–90.

Blaha C, Winn P (1993) Modulation of dopamine efflux in the striatum following cholinergic stimulation of the substantia nigra in intact and pedunculopontine tegmental nucleus-lesioned rats. J Neurosci 13:1035–1044.

Blaha C, Allen L, Das S, Inglis W, Latimer M, Vincent S, Winn P (1996) Modulation of dopamine efflux in the nucleus accumbens after cholinergic stimulation of the ventral tegmental area in intact, pedunculopontine tegmental nucleus-lesioned, and laterodorsal tegmental nucleus-lesioned rats. J Neurosci 16:714–722.

Bolam JP, Francis CM, Henderson Z (1991) Cholinergic input to dopaminergic neurons in the substantia nigra: a double immunocytochemical study. Neuroscience 41:483–494.

Boulter J, Connolly J, Deneris E, Goldman D, Heinemann S, Patrick J (1987) Functional expression of two neuronal nicotinic acetylcholine receptors from cDNA clones identifies a gene family. Proc Natl Acad Sci USA 84:7763–7767.

Bravo H, Karten HJ (1992) Pyramidal neurons of the rat cerebral cortex, immunoreactive to nicotinic acetylcholine receptors, project mainly to subcortical targets. J Comp Neurol 320:62–68.

Changeux JP (1991) Functional architecture and dynamics of the nicotinic acetylcholine receptor: an allosteric ligand-gated ion channel. Fidia Res Found Neurosci Award Lect 4:21–168.

Chen C, Okayama H (1987) High efficiency transfection of mammalian cells by plasmid DNA. Mol Cell Biol 7:2745–2752.

Clarke PBS, Pert A (1985) Autoradiographic evidence for nicotine receptors on nigrostriatal and mesolimbic dopaminergic neurons. Brain Res 348:355–358.

Clarke PBS, Hommer D, Pert A, Skirboll L (1985a) Electrophysiological actions of nicotine on substantia nigra single units. Br J Pharmacol 85:827–835.

Clarke PBS, Schwartz RD, Paul SM, Pert CB, Pert A (1985b) Nicotinic binding in rat brain: autoradiographic comparison of [^{3}H]acetylcholine, [^{3}H]nicotine, and ^{125}I-α-bungarotoxin. J Neurosci 5:1307–1315.

Clarke PBS, Hommer DW, Pert A, Skirboll LR (1987) Innervation of substantia nigra neurons by cholinergic afferents from pedunculopontine nucleus in the rat: neuroanatomical and electrophysiological evidence. Neuroscience 23:1011–1019.

Conroy WG, Berg DK (1995) Neurons can maintain multiple classes of nicotinic acetylcholine receptors distinguished by different subunit compositions. J Biol Chem 270:4424–4431.

Conroy WG, Vernallis AB, Berg DK (1992) The α5 product assembles with multiple acetylcholine receptor subunits to form distinctive receptor subtypes in brain. Neuron 9:679–691.

Corrigall WA, Franklin KBJ, Coen KM, Clarke PBS (1992) The mesolimbic dopaminergic system is implicated in the reinforcing effects of nicotine. Psychopharmacology 107:285–289.

Corringer PJ, Galzi J, Eisele J, Bertrand S, Changeux J, Bertrand D (1995) Identification of a new component of the agonist binding site of the nicotinic α7 homooligomeric receptor. J Biol Chem 270: 11749–11752.

Decarries L, Gisiger V, Steriade M (1997) Diffuse transmission by acetylcholine in the CNS. Prog Neurobiol 53:603–625.

Dehaene S, Changeux JP (1989) A simple model of prefrontal cortex function in delayed-response tasks. J Cognit Neurosci 1:244–261.

Dehaene S, Changeux JP (1997) A hierarchical neuronal network for planning behavior. Proc Natl Acad Sci USA 94:13293–13298.

Deneris ES, Boulter J, Swanson LW, Patrick J, Heinemann S (1989) β3: a new member of nicotinic acetylcholine receptor gene family is expressed in brain. J Biol Chem 264:6268–6272.

Deutch AY, Holliday J, Roth RH, Chun LLY, Hawrot E (1987) Immunohistochemical localization of a neuronal nicotinic receptor in mammalian brain. Proc Natl Acad Sci USA 84:8697–8701.

Dineley-Miller K, Patrick J (1992) Gene transcripts for the nicotinic acetylcholine receptor subunit, β4, are distributed in multiple areas of the rat central nervous system. Mol Brain Res 16:339–344.

Dominguez del Toro E, Juiz JM, Peng X, Lindstrom J, Criado M (1994) Immunocytochemical localization of the α7 subunit of the nicotinic acetylcholine receptor in the rat central nervous system. J Comp Neurol 349:325–342.

Duvoisin RM, Deneris ES, Patrick J, Heinemann S (1989) The functional diversity of the neuronal nicotinic acetylcholine receptors is increased by a novel subunits: β4. Neuron 3:487–496.

Eiselé JL, Bertrand S, Galzi JL, Devillers-Thiéry A, Changeux JP, Bertrand D (1993) Chimeric nicotinic-serotoninergic receptor combines distinct ligand binding and channel specificities. Nature 366:479–483.

Fallon JH, Loughlin SE (1995) Substantia nigra. In: The rat brain, Chap 12, Ed 2 (Paxinos G, ed), pp 215–237. San Diego: Academic.

Flores CM, Rogers SW, Pabreza LA, Wolfe BB, Kellar KJ (1992) A

subtype of nicotinic cholinergic receptor in rat brain is composed of α4-subunit and β2-subunit and is up-regulated by chronic nicotine treatment. Mol Pharmacol 41:31–37.

Futami T, Takakusaki K, Kitai ST (1995) Glutamatergic and cholinergic inputs from the pedunculopontine tegmental nucleus to dopamine neurons in the substantia nigra pars compacta. Neurosci Res 21:331–342.

Goldman D, Deneris E, Luyten W, Kochhar A, Patrick J, Heinemann S (1987) Members of a nicotinic acetylcholine receptor gene family are expressed in different regions of the mammalian central nervous system. Cell 48:965–973.

Goldner FM, Dineley KT, Patrick JW (1997) Immunohistochemical localization of the nicotinic acetylcholine receptor subunit α6 to dopaminergic neurons in the substantia nigra and ventral tegmental area. NeuroReport 8:2739–2742.

Gould E, Woolf NJ, Butcher LL (1989) Cholinergic projections to the substantia nigra from the pedunculopontine and laterodorsal tegmental nuclei. Neuroscience 28:611–623.

Griffiths G (1993) Fine structure immunocytochemistry. New York: Springer.

Happe HK, Peters JL, Bergman DA, Murrin LC (1994) Localization of nicotinic cholinergic receptors in rat brain: autoradiographic studies with [^{3}H]cytisine. Neuroscience 62:929–944.

Henderson Z, Greenfield SA (1987) Does the substantia nigra have a cholinergic innervation? Neurosci Lett 73:109–113.

Henderson Z, Sherriff FE (1991) Distribution of choline acetyltransferase immunoreactive axons and terminals in the rat and ferret brainstem. J Comp Neurol 314:147–163.

Hill JA, Zoli M, Bourgeois JP, Changeux JP (1993) Immunocytochemical localization of a neuronal nicotinic receptor: the β2 subunit. J Neurosci 13:1551–1568.

Horch HL, Sargent PB (1995) Perisynaptic surface distribution of multiple classes of nicotinic acetylcholine receptors on neurons in the chicken ciliary ganglion. J Neurosci 15:7778–7795.

Imperato A, Mulas A, Di Chiara G (1986) Nicotine preferentially stimulates dopamine release in the limbic system of freely moving rats. Eur J Pharmacol 132:337–338.

Jacob MH, Berg DK (1983) The ultrastructural localization of α-bungarotoxin binding sites in relation to synapses on chick ciliary ganglion neurons. J Neurosci 3:260–271.

Jacob MH, Berg DK, Lindstrom JM (1984) Shared antigenic determinant between the *Electrophorus* acetylcholine receptor and a synaptic component on chicken ciliary ganglion neurons. Proc Natl Acad Sci USA 81:3223–3227.

Koob GF (1992) Drugs of abuse: anatomy, pharmacology and function of reward pathways. Trends Pharmacol Sci 13:177–184.

Koob GF (1996) Drug addiction: the yin and yang of hedonic homeostasis. Neuron 16:893–896.

Le Novère N, Changeux JP (1995) Molecular evolution of the nicotinic acetylcholine receptor: an example of multigene family in excitable cells. J Mol Evol 40:155–172.

Le Novère N, Zoli M, Changeux JP (1996) Neuronal nicotinic receptor α6 subunit mRNA is selectively concentrated in catecholaminergic nuclei of the rat brain. Eur J Neurosci 8:2428–2439.

Lee H, Rye D, Hallanger A, Levey A, Wainer B (1988) Cholinergic vs. noncholinergic efferents from the mesopontine tegmentum to the extrapyramidal motor system nuclei. J Comp Neurol 275:469–492.

Levin ED (1992) Nicotinic systems and cognitive function. Psychopharmacology 108:417–431.

Levin ED, Rose JE (1995) Acute and chronic nicotinic interactions with dopamine systems and working memory performance. Ann NY Acad Sci 757:245–252.

Loring RH, Zigmond RE (1987) Ultrastructural distribution of ^{125}I-toxin-F binding sites on chick ciliary neurons: synaptic localization of a toxin that blocks ganglionic nicotinic receptors. J Neurosci 7:2153–2162.

Luetje CW, Patrick J (1991) Both α and β subunits contribute to the agonist sensitivity of neuronal nicotinic acetylcholine receptors. J Neurosci 11:837–845.

Luján R, Nusser Z, Roberts JD, Shigemoto R, Somogy P (1996) Perisynaptic location of metabotropic glutamate receptors mGluR1 and mGluR5 on dendrites and dendritic spines in the rat hippocampus. Eur J Neurosci 8:1488–1500.

Martinez-Murillo R, Villalba RM, Montero-Caballero MI, Rodrigo J (1989a) Cholinergic somata and terminals in the rat substantia nigra: an immunocytochemical study with optical and electron microscopic techniques. J Comp Neurol 281:397–416.

Martinez-Murillo R, Villalba RM, Rodrigo J (1989b) Electron microscopic localization of cholinergic terminals in the rat substantia nigra: an immunocytochemical study. Neurosci Lett 96:121–126.

Marubio LM, Arroyo-Jimenez MM, Cordero-Erausquin M, Léna C, LeNovère N, Benoit P, de Kerchove d'Exaerde A, Huchet M, Damaj MI, Changeux JP (1999) Reduced nicotine-elicited antinociception in mice lacking the neuronal α-4 nicotinic receptor subunit. Nature 398:805–810.

Mason WT (1985) Staining of magnocellular nuclei of the rat hypothalamus by a monoclonal antibody directed against the α-subunit of the nicotinic cholinergic receptor. Neurosci Lett 59:89–95.

Matsubara A, Laake JH, Davanger S, Usami S, Ottersen OP (1996) Organization of AMPA receptor subunits at a glutamate synapse: a quantitative immunogold analysis of hair cell synapses in the rat organ of Corti. J Neurosci 16:4457–4467.

Nagelhus EA, Veruki ML, Torp R, Haug FM, Laake JH, Nielsen S, Agre P, Ottersen OP (1998) Aquaporin-4 water channel protein in the rat retina and optic nerve: polarized expression in Muller cells and fibrous astrocytes. J Neurosci 18:2506–2519.

Nakayama H, Shioda S, Okuda H, Nakashima T, Nakai Y (1995) Immunocytochemical localization of nicotinic acetylcholine receptor in rat cerebral cortex. Mol Brain Res 32:321–328.

Nastuk M, Graybiel A (1991) Pharmacologically defined M1 and M2 muscarinic cholinergic binding sites in the cat's substantia nigra: development and maturity. Dev Brain Res 61:1–10.

Nisell M, Nomikos GG, Svensson TH (1994) Systemic nicotine-induced dopamine release in the rat nucleus accumbens is regulated by nicotinic receptors in the ventral tegmental area. Synapse 16:36–44.

Okuda H, Shioda S, Nakay Y, Nakayama H, Okamoto M, Nakashima T (1993) Immunocytochemical localization of nicotinic acetylcholine receptor in rat hypothalamus. Brain Res 625:145–151.

Orr-Urtreger A, Goldner FM, Saeki M, Lorenzo I, Goldberg L, De Biasi M, Dani JA, Patrick JW, Beaudet AL (1997) Mice deficient in the α7 neuronal nicotinic acetylcholine receptor lack α-bungarotoxin binding sites and hippocampal fast nicotinic currents. J Neurosci 17:9165–9171.

Paxinos G, Watson C (1986) The rat brain in stereotaxic coordinates. San Diego: Academic.

Paxinos G, Watson C, Emson P (1980) AChE-stained horizontal sections of the rat brain in stereotaxic coordinates. J Neurosci Methods 3:129–149.

Peters A, Palay S, de F Webster H (1991) The fine structure of the nervous system. Oxford: Oxford UP.

Picciotto M, Zoli M, Léna C, Bessis A, Lallemand Y, Le Novère N, Vincent P, Merlo-Pich E, Brulet P, Changeux JP (1995) Abnormal avoidance learning in mice lacking functional high-affinity nicotine receptor in the brain. Nature 374:65–67.

Picciotto M, Zoli M, Rimondini R, Léna C, Marubio LM, Merlo-Pich E, Fuxe K, Changeux JP (1998) Acetylcholine receptors containing the β2 subunit are involved in the reinforcing properties of nicotine. Nature 391:173–177.

Pidoplichko V, DeBiasi M, Williams J, Dani J (1997) Nicotine activates and desensitizes midbrain dopamine neurons. Nature 390:401–404.

Pontieri FE, Tanda G, Orzi F, Di Chiara G (1996) Effects of nicotine on the nucleus accumbens and similarity to those of addictive drugs. Nature 382:255–257.

Ragozzino D, Fucile S, Giovannelli A, Grassi F, Mileo AM, Ballivet M, Alema S, Eusebi F (1997) Functional properties of neuronal nicotinic acetylcholine receptor channels expressed in transfected human cells. Eur J Neurosci 9:480–488.

Ramirez-Latorre J, Yu CR, Qu X, Perin F, Karlin A, Role L (1996) Functional contributions of α5 subunit to neuronal acetylcholine receptor channels. Nature 380:347–351.

Rogers SW, Gahring LC, Collins AC, Marks M (1998) Age-related changes in neuronal nicotinic acetylcholine receptor subunit α4 expression are modified by long-term nicotine administration. J Neurosci 18:4825–4832.

Role LW, Berg DK (1996) Nicotinic receptors in the development and modulation of CNS synapses. Neuron 16:1077–1085.

Sargent PB (1993) The diversity of neuronal nicotinic acetylcholine receptors. Annu Rev Neurosci 16:403–443.

Scarnati E, Proia A, Campana E, Pacitti C (1986) A microiontophoretic study on the nature of the putative synaptic neurotransmitter involved

in the pedunculopontine-substantia nigra pars compacta excitatory pathway of the rat. Exp Brain Res 62:470–478.

Schroder H, Zilles K, Maelicke A, Hajos F (1989) Immunohisto- and cytochemical localization of cortical nicotinic cholinoceptors in rat and man. Brain Res 502:287–295.

Seguela P, Wadiche J, Dineley-Miller K, Dani JA, Patrick JW (1993) Molecular cloning, functional properties, and distribution of rat brain-α7. A nicotinic cation channel highly permeable to calcium. J Neurosci 13:596–604.

Sorenson EM, Shiroyama T, Kitai ST (1998) Postsynaptic nicotinic receptors on dopaminergic neurons in the substantia nigra pars compacta of the rat. Neuroscience 87:659–673.

Swanson LW, Simmons DM, Whiting PJ, Lindstrom J (1987) Immunohistochemical localization of neuronal nicotinic receptors in the rodent central nervous system. J Neurosci 7:3334–3342.

Tokuno H, Moriizumi T, Kudo M, Nakamura Y (1988) A morphological evidence for monosynaptic projections from the nucleus tegmenti pedunculopontinus pars compacta (TPC) to nigrostriatal projection neurons. Neurosci Lett 85:1–4.

Tzartos SJ, Rand DE, Einarson BL, Lindstrom J (1981) Mapping of surface structures of *Electrophorus* acetylcholine receptor using monoclonal antibodies. J Biol Chem 256:8635–8645.

Vernallis AB, Conroy WG, Berg DK (1993) Neurons assemble acetylcholine receptors with as many as three kinds of subunits while maintaining subunit segregation among receptor subtypes. Neuron 10:451–464.

Wada E, Wada K, Boulter J, Deneris E, Heinemann S, Patrick J, Swanson LW (1989) Distribution of α2, α3, α4, and β2 neuronal nicotinic receptor subunit mRNAs in the central nervous system: a hybridization histochemical study in the rat. J Comp Neurol 284:314–335.

Wada E, McKinnon D, Heinemann S, Patrick J, Swanson LW (1990) The distribution of mRNA encoded by a new member of the neuronal nicotinic acetylcholine receptor gene family (α5) in the rat central nervous system. Brain Res 526:45–53.

Wang F, Gerzanich V, Wells GB, Anand R, Peng X, Keyser K, Lindstrom J (1996) Assembly of human neuronal nicotinic receptor α5 subunits with α3, β2, and β4 subunits. J Biol Chem 271:17656–17665.

Whiting PJ, Lindstrom JM (1987) Purification and characterization of a nicotinic acetylcholine receptor from rat brain. Proc Natl Acad Sci USA 84:595–599.

Whiting PJ, Lindstrom JM (1988) Characterization of bovine and human neuronal nicotinic acetylcholine receptors using monoclonal antibodies. J Neurosci 8:3395–3404.

Woolf NJ, Butcher LL (1986) Cholinergic systems in the rat brain. III. Projections from the pontomesencephalic tegmentum to the thalamus, tectum, basal ganglia, and basal forebrain. Brain Res Bull 16:603–637.

Zoli M, Léna C, Picciotto M, Changeux JP (1998) Identification of four classes of brain nicotinic receptors using β2-mutant mice. J Neurosci 18:4461–4472.